

Blocking of Exchange Proteins Directly Activated by cAMP Leads to Reduced Replication of Middle East Respiratory Syndrome Coronavirus

Xinrong Tao,^a Feng Mei,^b Anurodh Agrawal,^a Clarence J. Peters,^{a,c,e,f} Thomas G. Ksiazek,^{c,d,e,f} Xiaodong Cheng,^{b*} Chien-Te K. Tseng^{a,c,e,f}

Departments of Microbiology and Immunology,^a Pharmacology and Toxicology,^b and Pathology,^d Center for Biodefense and Emerging Infectious Diseases,^c Sealy Center for Vaccine Development,^e and Center for Tropical Diseases,^f University of Texas Medical Branch, Galveston, Texas, USA

The outbreak of Middle East respiratory syndrome coronavirus (MERS-CoV) infections and diseases represents a potential threat for worldwide spread and requires development of effective therapeutic strategies. In this study, we revealed a novel positive function of an exchange protein directly activated by cyclic AMP 1 (cAMP-1; Epac-1) on MERS-CoV replication. Specifically, we have shown that Epac-specific inhibitor treatment or silencing Epac-1 gene expression rendered cells resistant to viral infection. We believe Epac-1 inhibitors deserve further study as potential therapeutic agents for MERS-CoV infection.

The outbreak of Middle East respiratory syndrome coronavirus (MERS-CoV) infections poses a threat to public health worldwide. MERS-CoV causes a severe acute respiratory syndrome (SARS)-like human respiratory disease; the infections emerged in Saudi Arabia in 2012 and subsequently spread to eight other countries in the Middle East and to Europe (1, 2). As of 6 October 2013, it has caused 136 confirmed human infections, including 58 deaths, a case fatality rate of 43% (<http://www.cdc.gov/coronavirus/mers/>). Although the predicted pandemic potential of MERS is low (3), an increase with further evolution of MERS-CoV in nature is of concern. To date, no effective treatment for infected individuals has been reported, indicating the need for development of effective therapeutic approaches.

Cyclic AMP (cAMP) is a regulator of many biological processes in many life forms, including microorganisms, plants, animals, and humans (4, 5). Intracellular levels of cAMP are tightly regulated by many cell type-specific isoforms of adenylyl cyclase (AC) and phosphodiesterase (PDE), a family of enzymes that inhibit cAMP signaling by degrading intracellular cAMP (6, 7). While the impact of cAMP on diverse cellular functions is complex, an elevated expression of intracellular cAMP generally suppresses host antimicrobial defense (8). A critical role for cAMP signaling in regulating host defense mechanisms is underscored by the fact that many pathogens, including viruses, establish infection in permissive hosts by having evolved strategies targeting the adenosine-cAMP axis to modulate the levels of intracellular cAMP (9).

Protein kinase A (PKA) and exchange proteins directly activated by cAMP (Epac) are two primary intracellular cAMP binding proteins that mediate most of the cAMP-regulated physiological functions (10–15). While most of the cAMP-mediated biological processes are classically associated with PKA, recent studies have indicated that Epac, acting either alone or in concert with PKA, regulates diverse biological responses by activating several members of the Ras superfamily, in particular Rap GTPase, via GTP loading (16). Epac exists as two isoforms, Epac-1 and Epac-2, which are coded by different genes. Alternative splicing adds to the complexity of the differential expression profile of

Epac both on the mRNA and protein levels (17). Specifically, Epac-1 is abundantly expressed in the heart, kidney, blood vessels, adipose tissue, central nervous system (CNS), ovary, uterus, and various myeloid and lymphoid cells, whereas Epac-2 sliced variants are mostly expressed in the CNS, adrenal gland, and pancreas (16). Although intracellular cAMP plays a role in regulating host antimicrobial responses, its effect on MERS-CoV infection in permissive cells has not been previously investigated.

We have recently shown that human bronchial epithelial Calu-3 cells are highly permissive to MERS-CoV, resulting in acute and profound apoptosis (18). Since PKA and Epac serve as key mediators of cAMP signaling, to investigate if cAMP signaling participates in regulating the infection of virus, we pretreated Calu-3 cells with either H89 (LC Laboratories), a PKA-specific inhibitor (19), an Epac-specific inhibitor (ESI-09) (13, 20), or dimethyl sulfoxide (DMSO) (as the carrier control) for 2 h before challenging the cells with MERS-CoV at a multiplicity of infection (MOI) of 0.1. Subsequent effects on infected cells were assessed by monitoring the formation of cytopathic effects (CPE) and the yields of infectious progeny virus at 24 h postinfection (p.i.). We found that prior treatment with ESI-09, but not H89, attenuated CPE formation (data not shown) and significantly reduced viral yields ($P < 0.001$) (Fig. 1A). To determine if ESI-09-mediated inhibition of MERS-CoV replication is limited to Calu-3 cells, we performed the same experiment using Vero E6 cells. Figure 1B

Received 11 October 2013 Accepted 17 December 2013

Published ahead of print 22 January 2014

Editor: S. Perlman

Address correspondence to Chien-Te K. Tseng, sktseng@utmb.edu, or Xiaodong Cheng, xiaodong.cheng@uth.tmc.edu.

* Present address: Xiaodong Cheng, Department of Integrative Biology and Pharmacology, The University of Texas Health Science Center, Houston, Texas, USA.

Copyright © 2014, American Society for Microbiology. All Rights Reserved.

doi:10.1128/JVI.03001-13

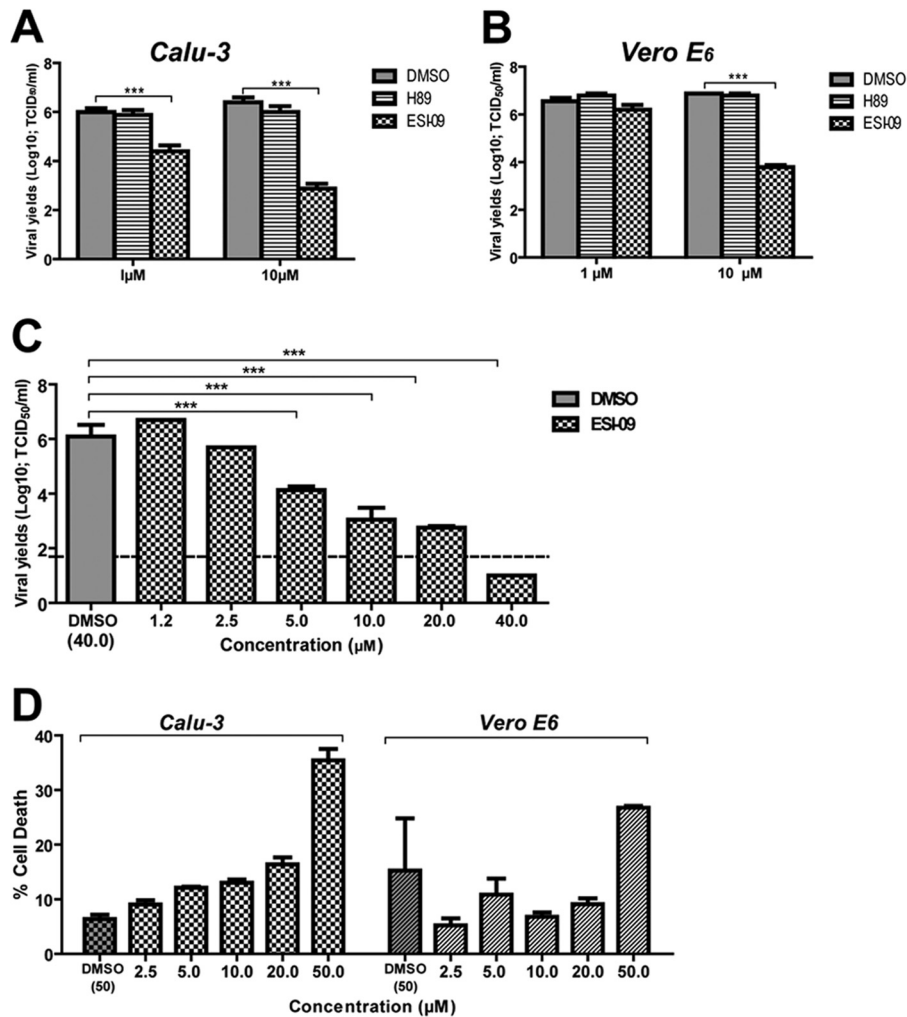


FIG 1 Prior treatment with ESI-09, but not H89, protects permissive cells against MERS-CoV infection in a cell type-independent manner. Confluent Calu-3 cells were treated with DMSO (as the control), H89, or ESI-09, all at 1 and 10 μ M, for 2 h before MERS-CoV challenge at an MOI of 0.1. (A) The effect of the different treatments on viral yield was evaluated at 24 h pi. (B) Similar experiments were also performed using Vero E6 cells. (C) The effective concentrations of ESI-09 were determined by treating Calu-3 cells as described in panel A with serial 2-fold dilutions of ESI-09 and comparing yields of infectious virus at 24 h (MOI of 0.1). (D) The lactate dehydrogenase (LDH)-based cytotoxicity assay (Promega) was used to evaluate the drug's cytotoxic potential. Briefly, confluent Calu-3 and Vero E6 cells grown in 6-well plates were incubated with the indicated concentrations of ESI-09 for 24 h before LDH released into the culture medium was assessed. Cells incubated with 50 μ M DMSO were included as controls. ***, $P < 0.001$, 1-way or 2-way analysis of variance (ANOVA). A representative from at least two independently conducted experiments of each type is presented.

indicates that the ability of ESI-09 treatment to restrict MERS-CoV infection was cell type independent, as results were similar with Vero E6 cells. We also noted that a significant reduction in virus yield occurred when cells were treated with ESI-09 at the concentrations between 5 and 40 μ M in Calu-3 cells (Fig. 1C). As shown in Fig. 1D, the concentration of ESI-09 required for causing 50% inhibition of cell survival (CC_{50}) was greater than 50 μ M for both Calu-3 and Vero E6 cells, based on the lactate dehydrogenase (LDH)-based cytotoxicity assay (Promega), suggesting that the anti-MERS-CoV growth inhibition imposed by ESI-09 treatment at the concentration of 10 μ M was not because of drug cytotoxicity. To further investigate the effect of ESI-09 on MERS-CoV replication, Calu-3 cells grown in 8-well chamber slides (Nunc Lab-Tek) were treated with 10 μ M H89, ESI-09, or DMSO for 2 h prior to challenge with virus at an MOI of 0.1. The effect of ESI-09 was assessed by determining the yields of infectious virus and the ex-

pressions of CD26, the receptor of MERS-CoV (21), and virus-specific antigens at 24 h p.i. by the standard indirect immunofluorescence (IIF) staining. Stained specimens were analyzed with an inverted UV microscopy (Olympus 1X51). As shown in Fig. 2A, DMSO control and H89 treatment did not protect against MERS-CoV infection, as shown by the extensive CPE (i.e., detachment of monolayer) and readily detectable viral antigen (red). In contrast, Calu-3 cells treated with ESI-09 were almost fully protected, as indicated by unnoticeable CPE and minimal expression of viral antigen. This capacity of ESI-09 to protect cells against MERS-CoV infection was consistent with the amount of infectious progeny viruses detected (Fig. 2B). To evaluate whether the anti-MERS-CoV activity of ESI-09 could be extended to include anti-SARS-CoV activity, we performed experiments using the same treatment and infection strategy as described for MERS-CoV. Prior ESI-09, but not H89, treatment was also effective in protect-

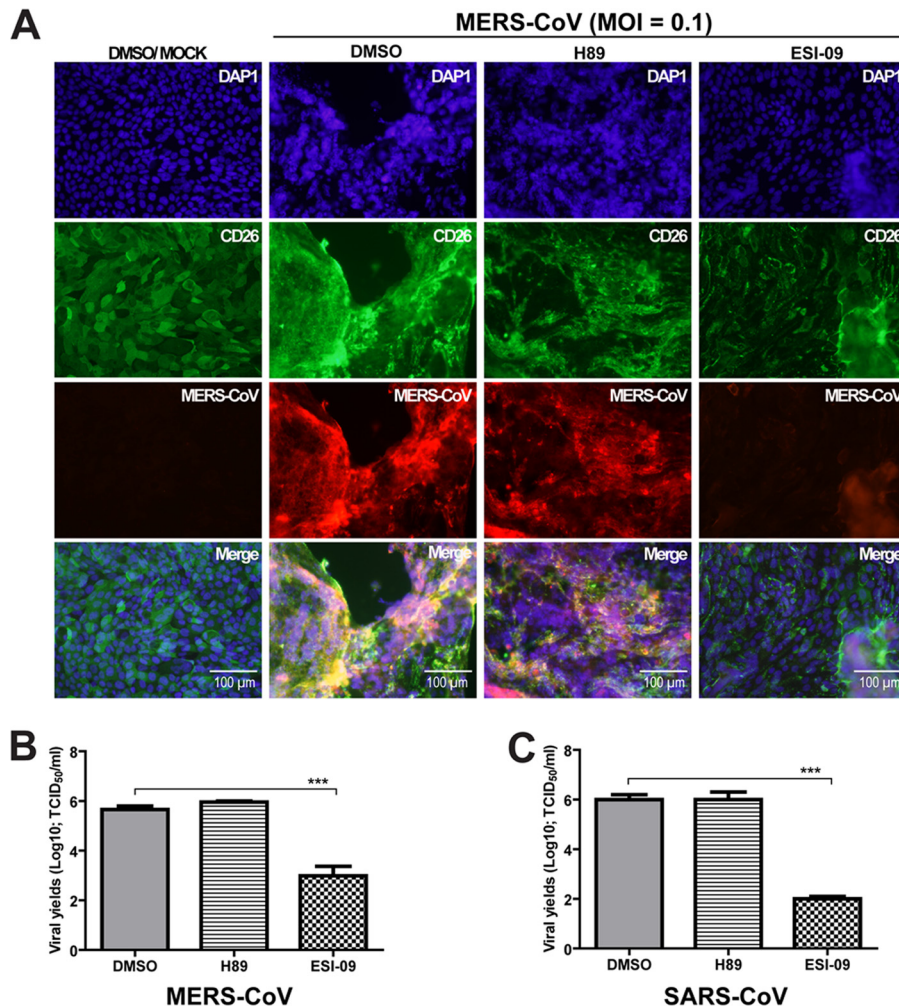


FIG 2 Prior ESI-09 treatment is as effective in protecting Calu-3 cells against both MERS-CoV and SARS-CoV. Calu-3 cells grown in chamber slides were pretreated with 10 μ M DMSO, H89, or ESI-09 for 2 h, followed by infection with MERS-CoV (MOI of 0.1) for 24 h before assessing the expressions of CD26 and virus-specific antigen in infected versus mock-infected cultures by indirect immunofluorescent (IIF) staining. Briefly, paraformaldehyde (4%)-fixed infected Calu-3 cells were stained with goat anti-human CD26 (5 mg/ml; R&D) and rabbit anti-MERS-CoV (1:200 dilution) antibodies (a generous gift from Heinz Feldmann; NIH/Rocky Mountain Laboratories, Hamilton, MT), followed by staining with either Alex488-conjugated donkey anti-goat IgG or Alex568-conjugated donkey anti-rabbit IgG. DAPI (4',6-diamidino-2-phenylindole) was used to stain the nucleus of cells. (A) Stained cultures were analyzed by using an inverted phase contrast fluorescence microscope (Olympus IX51). (B) Cell-free supernatants harvested at 24 h p.i. were used to determine the yields of MERS-CoV. Confluent Vero E6 cells grown in 12-well plates were similarly subjected to treatment with 10 μ M DMSO, H89, or ESI-09 prior to infection with SARS-CoV (MOI of 0.1), followed by assessing the yield of virus in culture medium at 24 h p.i. ***, $P < 0.001$, 1-way ANOVA. A representative from at least three independently conducted experiments is presented.

ing cell cultures against SARS-CoV, resulting in nearly a 4- \log_{10} reduction in viral titers (Fig. 2C).

As the extracellular domain of CD26 can be released into the circulation as soluble CD26 (22, 23), we investigated whether ESI-09 treatment might reduce surface expression of CD26, thereby reducing MERS-CoV binding and subsequent virus replication. For this, we compared the effect of DMSO versus ESI-09 treatment, at 10 μ M for 2 h, on CD26 expression in Calu-3 cells by both Western blotting and IIF. Whereas the total amount of CD26 was not affected by ESI-09 treatment (Fig. 3A), the pattern of CD26 expression on the membrane of Calu-3 cells was changed with ESI-09 treatment (Fig. 3B). In contrast to the relatively diffuse expression pattern in DMSO-treated cells, the expression of CD26 was rearranged, becoming more concentrated at the cell membrane in response to ESI-09 treatment. We also investigated

whether such an altered pattern of CD26 expression would affect viral binding to Calu-3 cells. For this study, we incubated untreated or DMSO-, H89-, or ESI-09-treated Calu-3 cells with an equal amount of infectious MERS-CoV (MOI of 20) in an ice bath for 2 h; cells were then washed thoroughly with ice-cold phosphate-buffered saline (PBS) to remove unbound viruses and submitted to one cycle of freeze (-80°C)-thaw in 100 μ l of minimal essential medium (MEM)-2% fetal calf serum (FCS) medium to maximally retrieve membrane-bound viral particles for titrations. As shown in Fig. 3C, neither H89 nor ESI-09 treatment adversely influenced MERS-CoV binding to Calu-3 cells, compared to untreated or DMSO-treated cells. To identify which stage(s) of a virus's life cycle downstream of the binding/adsorption might be affected by ESI-09 treatment, Calu-3 cells grown in 12-well plates were infected with live or gamma (γ)-inactivated (cobalt-60, 5

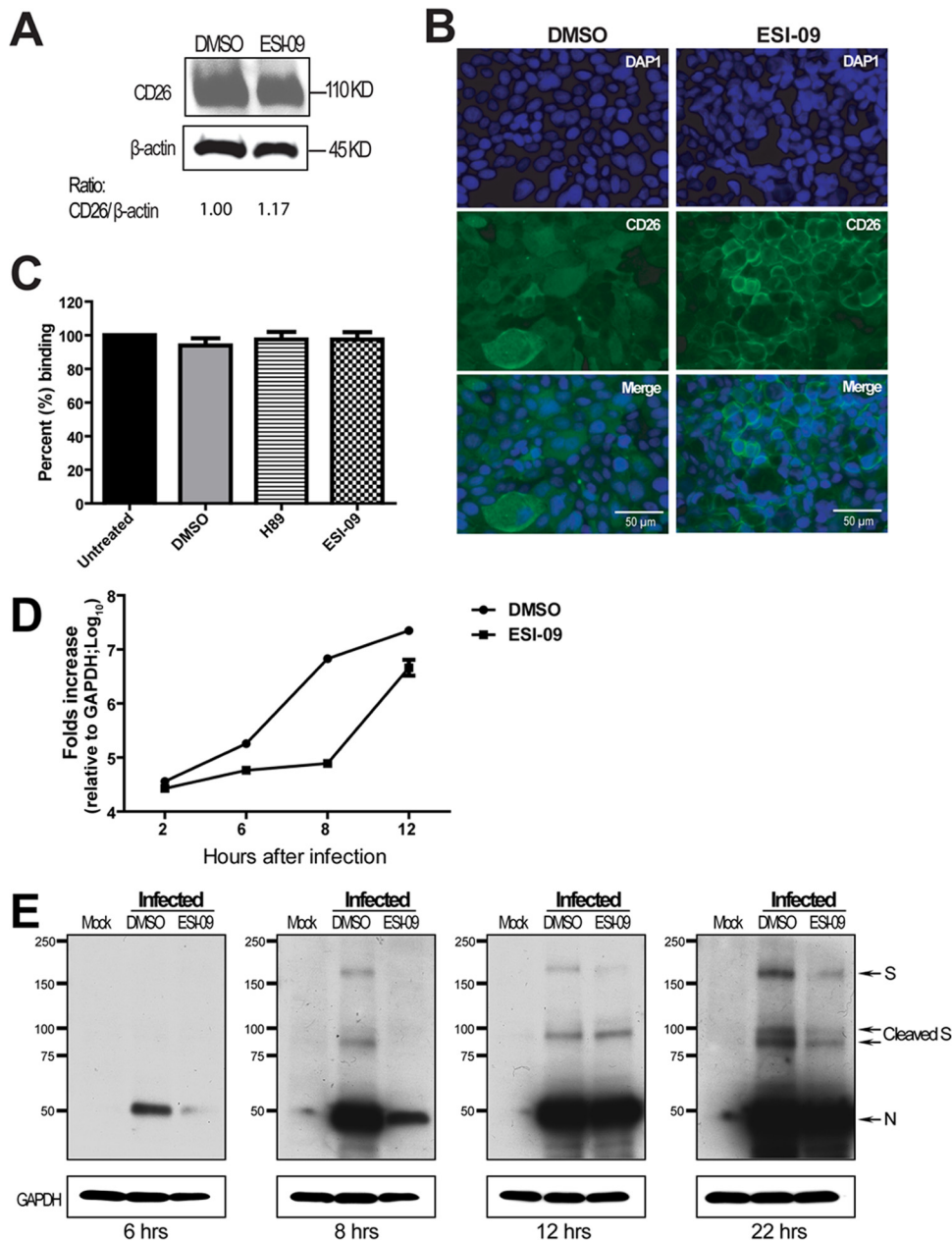


FIG 3 ESI-09 treatment is effective in inhibiting viral RNA replication and protein expression of MERS-CoV without affecting total CD26 expression and virus binding to Calu-3 cells. The amount of CD26 glycoprotein in the lysates of Calu-3 cells treated for 2 h with either 10 μ M DMSO or ESI-09 was determined by Western blotting. Constitutively expressed β -actin was included as an internal control. (A) The resulting protein bands were analyzed using ImageJ, and the ratios between the densities of CD26 and β -actin within each cell type were compared for the effect of different treatments on CD26 expression. The expression of CD26 in Calu-3 cells treated with 10 μ M DMSO or ESI-09 for 24 h was also monitored by IIF staining with goat anti-human CD26/DPP4 antibodies and Alexa 488-conjugated donkey anti-goat immunoglobulin, as indicated in the text. DAPI staining of cellular nuclei was included (blue). (B) The cultures were analyzed by using an inverted phase contrast fluorescence microscope (Olympus IX51). The binding efficiencies of MERS-CoV on the membranes of untreated and treated Calu-3 cells were evaluated as described in the text. Briefly, the differentially treated cells were incubated with MERS-CoV (MOI of 20) in an ice bath for 2 h, washed thoroughly with ice-cold PBS, and subjected to 1 cycle of freeze-thaw before the titers of membrane-bound viral particles were determined in Vero E6-based infection assays. (C) Virus binding to untreated Calu-3 cells was defined as 100%. A representative of at least two independently conducted experiments to each subset of the study is presented. The effects of ESI-09 treatment on viral RNA replication and protein expression over time were also evaluated. Briefly, Calu-3 cells challenged with live or γ -inactivated MERS-CoV (MOI = 5) were treated with DMSO or ESI-09 (10 μ M) for the indicated time points p.i. before subjecting to total RNA extraction and cell lysate preparation. Quantitative RT-PCR (qRT-PCR) analyses targeting virus-specific upstream E gene and cellular GAPDH gene (as the endogenous control) were used to monitor the kinetics of RNA replication. (D) The intensity of the mRNA of the upstream E gene of each sample relative to that of GAPDH was calculated according to the standard threshold cycle ($\Delta\Delta C_T$) method (37), and the average of mRNA signaling in duplicate samples is depicted. (E) For determining the effect of ESI-09 treatment on the viral protein synthesis, Western blot analyses with a pair of rabbit anti-MERS-CoV antibodies (1:2,000) and horseradish peroxidase (HRP)-conjugated goat anti-rabbit IgG (1:15,000; Cell Signaling Technology) were employed.

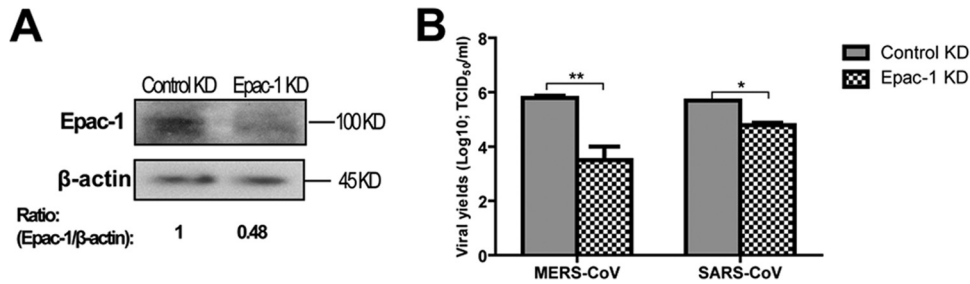


FIG 4 Epac-1 gene knockdown (KD) results in a significantly reduced susceptibility of Calu-3 cells in response to both MERS-CoV and SARS-CoV infection. The phenotypes of stable Epac-1 KD and control KD Calu-3 cells, established by shRNA lentiviral transduction, were determined by Western blotting analyses. Epac-1 contents were compared, using the ratios of relative densities between protein bands of Epac-1 and β -actin (as the control) as measured by ImageJ. (A) The ratio between Epac-1 and β -actin in control KD cells was defined as 1. The impact of Epac-1 KD on MERS-CoV and SARS-CoV replication was assessed after infection with each of the viruses at an MOI of 0.1 for 24 h. (B) The resulting virus yields were assessed by Vero E6-based infection assays. **, $P < 0.01$; *, $P < 0.05$; 2-way ANOVA. A representative from three independently conducted experiments is presented.

megarads) MERS-CoV (MOI = 5) for 1 h at 4°C, followed by ESI-09 or DMSO treatment (10 μ M), before harvesting total RNA and cell lysates at the indicated time points p.i. for determining the kinetics of virus RNA replication by using a real-time (RT) reverse transcription touch thermal cycler (Bio-Rad) and Western blot analyses. For quantifying viral RNA replication by RT-PCR, we targeted a region upstream of the envelope (E) gene (*upE*), as described previously (24), and the GAPDH gene as the internal control. As shown in Fig. 3D, ESI-09 treatment significantly inhibited genomic replication of virus, starting at 6 h, reaching the maximum at 8 h, and remained inhibitory at 12 h p.i. As anticipated, viral RNA replication was not detected in cells challenged with γ -inactivated virus (data not shown). These ESI-09-mediated inhibitory kinetics of viral RNA replication was consistent with the expression of spike-surface glycoproteins (S) and the nucleocapsid (N) protein as revealed by Western blot analyses (Fig. 3E), thereby suggesting that inhibiting viral RNA replication and protein synthesis are likely antiviral mechanisms of ESI-09. Taken together, these results suggested that the cAMP-Epac, but not cAMP-PKA, signaling axis plays a role in the regulation of MERS-CoV replication in permissive cells.

To more definitely demonstrate that Epac proteins are important for sustaining viral replication, we established Epac-1 gene knockdown (KD) Calu-3 cells by using the short hairpin RNA (shRNA) lentiviral transduction system (Sigma-Aldrich) (25). These KD cells enabled us to examine the effect Epac-1 might have in regulating the replication of both MERS-CoV and SARS-CoV and to validate the results attributed to the pharmacological inhibitor. As shown in Fig. 4A, Epac-1 expression was reduced by ~50% in KD Calu-3 cells compared to that in the control KD cells. To evaluate whether such a moderate reduction in Epac-1 expression could have an effect on viral replication similar to that of the ESI-09 treatment, we infected both control and Epac-1 KD cells with either MERS-CoV or SARS-CoV (MOI of 0.1) for 24 h before assessing virus yields. As shown in Fig. 4B, reducing Epac-1 expression by ~50% was sufficient to significantly reduce the replication of MERS-CoV and SARS-CoV.

While the activity state of Epac, a multidomain mediator of cAMP signaling, is determined by its allosteric interaction with cAMP (16), an increased transcriptional expression of Epac gene has been demonstrated in mice suffered from either myocardial hypertrophy or neointima formation induced by vascular injury

(26, 27). Since Epac appears to play a previously unidentified role in supporting viral replication, we determined whether its expression could be modified in response to acute MERS-CoV infection. Briefly, MERS-CoV-infected Calu-3 cells (MOI = 5) grown in 12-well plates were treated with DMSO or ESI-09 (10 μ M) for the indicated time periods before harvesting supernatants and extracting cellular lysates for assessing virus titers and Epac protein expression. As anticipated, early ESI-09 treatment resulted in profound reduction of virus titers, especially at both 12 and 22 h p.i. (data not shown). Western blot analyses using mouse anti-Epac (Santa Cruz) or rabbit anti-GAPDH antibody (Cell Signaling Technology) in combination of anti-mouse IgG-horseradish peroxidase (HRP) (Biolab) or anti-rabbit IgG-HRP (Cell Signaling Technology) revealed that neither ESI-09 treatment nor MERS-CoV infection over time could significantly modulate the level of Epac protein expression (Fig. 5A). We also determined if the expression of Epac can be colocalized with intracellular virus, in which Calu-3 cells grown in chamber slides were infected with recombinant MERS-CoV (rMERS-CoV) expressing red fluorescence protein (RFP) at 4°C for 1 h (28), followed by treatment with either DMSO or ESI-09 for the indicated time periods before assessing the expression of Epac and MERS-CoV-RFP by IF. Consistent with Western blot results, the expression pattern and intensity of Epac (Fig. 5B, green dots, arrows) in Calu-3 cells was not affected by either MERS-CoV infection or ESI-09 treatment. Additionally, its expression was not strictly colocalized with intracellular viruses either (Fig. 5B, red, arrowheads).

While it is clear that prior ESI-09 treatment was effective in restricting MERS-CoV and SARS-CoV replication without compromising viral binding, we further evaluated whether the antiviral effect provided by ESI-09 could be attributed to a virucidal effect. For this test, we incubated an equal volume of SARS-CoV or MERS-CoV with MEM-2% FCS (M-2), DMSO (10 μ M), or ESI-09 (10 μ M) at 37°C for 2 h before determining their effect on viral yields in Vero E6 cells. We found that neither DMSO nor ESI-09 treatment had any noticeable direct effect on the resulting viral yields (Fig. 6A). To investigate if the antiviral effect of ESI-09 required its continuing presence in the culture system, we treated duplicate sets of Calu-3 cell cultures with DMSO vehicle or 10 μ M ESI-09 for 2 h. One set was replenished with DMSO and ESI-09 after MERS-CoV challenge (MOI of 0.1), whereas the other set received M-2 medium without the additives. As shown in Fig. 6B,

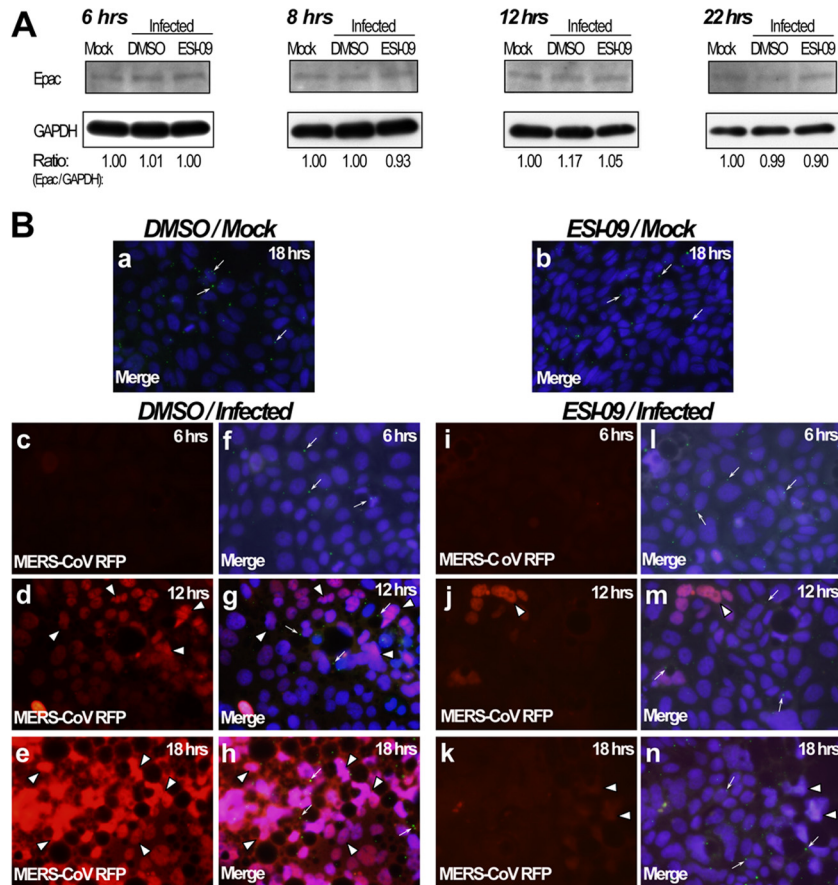


FIG 5 Neither ESI-09 treatment nor MERS-CoV infection affects the expression and localization of Epac protein in Calu-3 cells. Calu-3 cells grown either in 12-well plates or in chamber slides were infected with MERS-CoV or rMERS-CoV-RFP (MOI = 5) for 1 h, followed by DMSO or ESI-09 treatment (10 μ M) for 6, 8, 12, 18, and/or 22 h before assessing the expression and localization of Epac protein. Specifically, Western blot analyses of the expression levels of Epac protein in response to DMSO and ESI-09 treatment and MERS-CoV infection over time were compared, using the ratios of relative densities between protein bands of Epac and GAPDH (as control) as measured by ImageJ. The ratio between Epac and GAPDH in mock-infected controls at each time point was defined as 1. For localizing the expression of Epac protein and MERS-CoV-RFP replication, indirect IF staining was used. Briefly, the Epac protein in differentially treated cells was revealed by using a pair of anti-Epac and its isotype-matching Alexa 488-conjugated secondary antibodies, whereas direct IF was used to directly assess the replication of MERS-CoV-RFP, a generous gift of Amy Sims and Ralph Baric (University of North Carolina, Chapel Hill, NC), under an inverted phase contrast fluorescence microscope (Olympus IX51). DAPI was used to stain the nucleus of cells (blue). Epac expression (green, arrow) in uninfected, DMSO-treated (a) or ESI-09-treated (b) cells, MERS-CoV-RFP expression (red, arrowhead) in DMSO-treated (c to e) or ESI-09-treated (i to k) cells, merged Epac and MERS-CoV-RFP expression in DMSO-treated (f to h) or ESI-09-treated (l to n) cells. A representative from two independently performed experiments is presented. Magnification, \times 400.

the ability of ESI-09 to inhibit viral replication appears to be reversible, as cells first treated with ESI-09 and replenished with M-2 medium without ESI-09 showed no evidence of virus inhibition. Finally, to determine if treatment of cells prior to challenge is a prerequisite for ESI-09's antiviral effect, we examined the effect of adding ESI-09 at various times after initiating virus infection. Briefly, Calu-3 cells were treated with ESI-09 at the indicated time points (Fig. 6C and D), where 0 h is defined as the time of viral challenge. Cell culture supernatants were harvested for assessing protective efficacy at either 38 h (MOI of 0.1) or 24 h (MOI of 5) postchallenge. Not only was the prechallenge treatment unnecessary for protection, but treating infected cells (MOI of 0.1) with ESI-09 as late as 16 or 20 h (Fig. 6C) or treating 12 h postchallenge for those infected with an MOI of 5 (Fig. 6D) was effective in reducing viral replication, thereby suggesting the treatment late in infection could be beneficial. The effectiveness of such a delayed ESI-09 treatment in plunging the yields of virus in Calu-3 cells

suggests that this antiviral drug might affect a late event(s) of the virus replication strategy, such as assembly and/or release, in addition to inhibiting synthesis of viral proteins and RNA replication (Fig. 3D and E).

In summary, in these initial studies of the potential linkage of the cAMP signaling pathway and MERS-CoV infection, we identified a previously unknown function of Epac-1 protein in regulating the replication of both MERS-CoV and SARS-CoV in a cell type-independent manner. These conclusions were based on the usage of both an Epac-specific inhibitor (ESI-09) and Epac-1 KD cells and Calu-3 and Vero E6 tissue cultures. While the exact mechanism of the cAMP-Epac axis in the cellular events of viral replication remains to be fully described, we found that ESI-09 exerts an antiviral effect when used at a nontoxic concentration. In addition, it does so, not only without the need for treatment prior to infection, but also with an extended therapeutic window. Incidentally, adenosine and its analogs have been successfully investi-

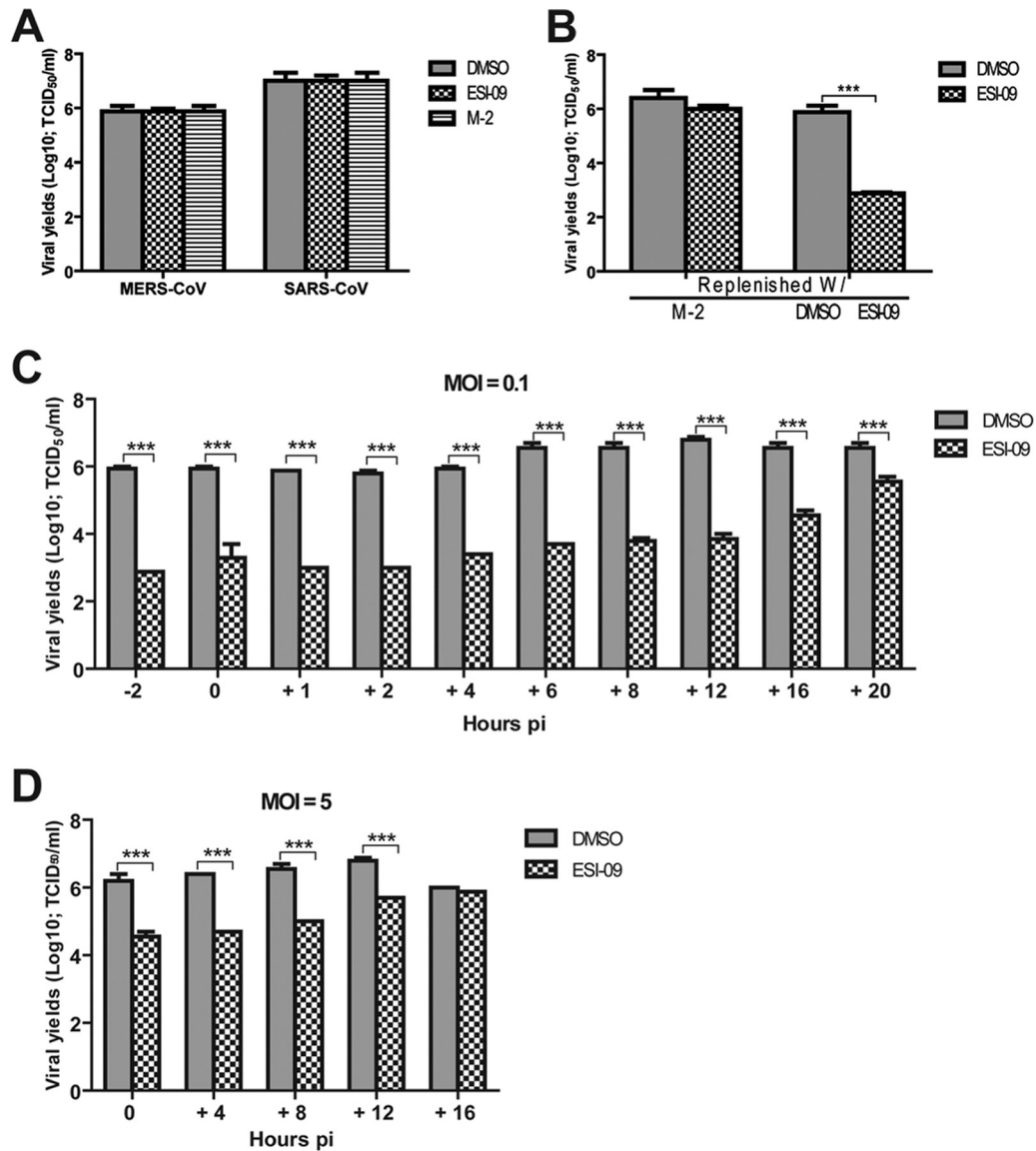


FIG 6 ESI-09 is not virucidal, possesses an unusual wide and effective therapeutic window, and requires its continual presence in the infected cultures to be effective against both MERS-CoV and SARS-CoV infection in Calu-3 cells. Equal aliquots of MERS-CoV or SARS-CoV stocks were incubated at 37°C for 2 h with an equal volume of MEM-2% fetal calf serum (FCS) medium or 20 μ M either DMSO or ESI-09 for a final concentration of 10 μ M each. (A) The infectious virus yield was subsequently determined by Vero E6-based infection assays. To evaluate the duration of ESI-09 treatment needed to protect against MERS-CoV infection in Calu-3 cells, two sets of duplicate cell cultures were treated with 10 μ M DMSO or ESI-09 for 2 h. After challenge with MERS-CoV (MOI of 0.1), one set was replenished with DMSO and ESI-09, respectively, whereas the other set was replenished with M-2 medium. (B) The resulting supernatants were tested for virus yield at 24 h p.i. To examine the therapeutic potential of ESI-09, confluent Calu-3 cells grown in 12-well plates were treated with ESI-09 (10 μ M) or DMSO at the indicated time points, where 0 h is defined as the time of MERS-CoV infection (MOIs of 0.1 and 5). The yield of progeny virus was assessed at 38 h (MOI of 0.1) (C) or 24 h (MOI of 5) (D) p.i., as described elsewhere, and was used to evaluate the therapeutic potential. ***, $P < 0.001$, 2-way ANOVA. A representative from two independently conducted experiments is presented.

gated as potent inhibitors of the replication of hepatitis C virus, vaccinia virus, HIV-1, dengue virus, and other flaviviruses (29–32). The dual role of CD26 as the MERS-CoV receptor and an adenosine deaminase (ADA)-anchoring protein (33–36) provides a potential linkage between MERS-CoV infection and cAMP signaling. However, the potential role of the cAMP axis in the host response to MERS-CoV has yet to be studied. Nevertheless, these findings indicate that further characterization and development of ESI-09 and its analogs as a new class of antiviral agents may

represent a strategy for combating MERS-CoV and possibly other emerging and reemerging virus infections.

ACKNOWLEDGMENTS

We thank Heinz Feldmann, National Institutes of Health, Hamilton, MT, Ron A. Fouchier, Erasmus Medical Center, Rotterdam, The Netherlands, and Amy Sims and Ralph Baric, University of North Carolina, Chapel Hill, NC, for providing MERS-CoV and virus-specific antibody and rMERS-CoV-RFP virus for our study and Mardelle Susman for her editorial assistance with the

manuscript. Special thanks go to Robert Couch, Baylor College of Medicine, for his critical reading of and excellent comments about the manuscript.

This study was supported, in part, by residual funds and a pilot grant from the Center for Biodefense and Emerging Infectious Diseases, University of Texas Medical Branch, Galveston, TX, awarded to C.-T.K.T. and by National Institutes of Health grants (R01GM066170 and R01GM106218) awarded to X.C.

REFERENCES

- WHO. 2013. Middle East respiratory syndrome coronavirus (MERS-CoV) summary and literature update. WHO, Geneva, Switzerland. http://www.who.int/csr/disease/coronavirus_infections/update_2013_0813/en.
- Breban R, Riou J, Fontanet A. 2013. Interhuman transmissibility of Middle East respiratory syndrome coronavirus: estimation of pandemic risk. *Lancet* 382:694–699. [http://dx.doi.org/10.1016/S0140-6736\(13\)61492-0](http://dx.doi.org/10.1016/S0140-6736(13)61492-0).
- Assiri A, Al-Tawfiq JA, Al-Rabeeh AA, Al-Rabiah FA, Al-Hajjar S, Al-Barrak A, Flemban H, Al Nassir WN, Balkhy HH, Al-Hakeem RF, Makhdoom HQ, Zumla AI, Memish ZA. 2013. Epidemiological, demographic, and clinical characteristics of 47 cases of Middle East respiratory syndrome coronavirus disease from Saudi Arabia: a descriptive study. *Lancet Infect. Dis.* 13:752–761. [http://dx.doi.org/10.1016/S1473-3099\(13\)70204-4](http://dx.doi.org/10.1016/S1473-3099(13)70204-4).
- Serezani CH, Ballinger MN, Aronoff DM, Peters-Golden M. 2008. Cyclic AMP: master regulator of innate immune cell function. *Am. J. Respir. Cell Mol. Biol.* 39:127–132. <http://dx.doi.org/10.1165/rcmb.2008-0091TR>.
- Berdeaux R, Stewart R. 2012. cAMP signaling in skeletal muscle adaptation: hypertrophy, metabolism, and regeneration. *Am. J. Physiol. Endocrinol. Metab.* 303:E1–E17. <http://dx.doi.org/10.1152/ajpendo.00555.2011>.
- Hanoune J, Defer N. 2001. Regulation and role of adenylyl cyclase isoforms. *Annu. Rev. Pharmacol. Toxicol.* 41:145–174. <http://dx.doi.org/10.1146/annurev.pharmtox.41.1.145>.
- Willoughby D, Cooper DM. 2008. Live-cell imaging of cAMP dynamics. *Nat. Methods* 5:29–36. <http://dx.doi.org/10.1038/nmeth1135>.
- Beavo JA, Brunton LL. 2002. *Nat. Rev. Mol. Cell Biol.* Cyclic nucleotide research—still expanding after half a century. 3:710–718. <http://dx.doi.org/10.1038/nrm911>.
- McDonough KA, Rodriguez A. 2011. The myriad roles of cyclic AMP in microbial pathogens: from signal to sword. *Nat. Rev. Microbiol.* 10:27–38. <http://dx.doi.org/10.1038/nrmicro2688>.
- Dekkers BG, Racké K, Schmidt M. 2013. Distinct PKA and Epac compartmentalization in airway function and plasticity. *Pharmacol. Ther.* 137: 248–265. <http://dx.doi.org/10.1016/j.pharmthera.2012.10.006>.
- Grandoch M, Roscioni SS, Schmidt M. 2010. The role of Epac proteins, novel cAMP mediators, in the regulation of immune, lung and neuronal function. *Br. J. Pharmacol.* 159:265–284. <http://dx.doi.org/10.1111/j.1476-5381.2009.00458.x>.
- Stork PJ, Schmitt JM. 2002. Crosstalk between cAMP and MAP kinase signaling in the regulation of cell proliferation. *Trends Cell Biol.* 12:258–266. [http://dx.doi.org/10.1016/S0962-8924\(02\)02294-8](http://dx.doi.org/10.1016/S0962-8924(02)02294-8).
- Almahariq M, Tsalkova T, Mei FC, Chen H, Zhou J, Sastry SK, Schwede F, Cheng X. 2013. A novel EPAC-specific inhibitor suppresses pancreatic cancer cell migration and invasion. *Mol. Pharmacol.* 83:122–128. <http://dx.doi.org/10.1124/mol.112.080689>.
- Ji Z, Mei FC, Cheng X. 2010. Epac, not PKA catalytic subunit, is required for 3T3-L1 preadipocyte differentiation. *Front. Biosci.* 2:392–398.
- Cheng X, Ji Z, Tsalkova T, Mei F. 2008. Epac and PKA: a tale of two intracellular cAMP receptors. *Acta Biochim. Biophys. Sin. (Shanghai)* 40: 651–662. <http://dx.doi.org/10.1111/j.1745-7270.2008.00438.x>.
- Schmidt M, Dekker FJ, Maarsingh H. 2013. Exchange protein directly activated by cAMP (epac): a multidomain cAMP mediator in the regulation of diverse biological functions. *Pharmacol. Rev.* 65:670–709. <http://dx.doi.org/10.1124/pr.110.003707>.
- Niimura M, Miki T, Shibasaki T, Fujimoto W, Iwanaga T, Seino S. 2009. Critical role of the N-terminal cyclic AMP-binding domain of Epac2 in its subcellular localization and function. *J. Cell. Physiol.* 219:652–658. <http://dx.doi.org/10.1002/jcp.21709>.
- Tao X, Hill TE, Morimoto C, Peters CJ, Ksiazek TG, Tseng CT. 2013. Bilateral entry and release of Middle East respiratory syndrome coronavirus induces profound apoptosis of human bronchial epithelial cells. *J. Virol.* 87:9953–9958. <http://dx.doi.org/10.1128/JVI.01562-13>.
- Marunaka Y, Niisato N. 2003. H89, an inhibitor of protein kinase A (PKA), stimulates Na⁺ transport by translocating an epithelial Na⁺ channel (ENaC) in fetal rat alveolar type II epithelium. *Biochem. Pharmacol.* 66:1083–1089. [http://dx.doi.org/10.1016/S0006-2952\(03\)00456-8](http://dx.doi.org/10.1016/S0006-2952(03)00456-8).
- Tsalkova T, Mei FC, Li S, Chepurny OG, Leech CA, Liu T, Holz GG, Woods VL, Jr, Cheng X. 2012. Isoform-specific antagonists of exchange proteins directly activated by cAMP. *Proc. Natl. Acad. Sci. U. S. A.* 109: 18613–18618. <http://dx.doi.org/10.1073/pnas.1210209109>.
- Raj VS, Mou H, Smits SL, Dekkers DH, Müller MA, Dijkman R, Muth D, Demmers JA, Zaki A, Fouchier RA, Thiel V, Drosten C, Rottier PJ, Osterhaus AD, Bosch BJ, Haagmans BL. 2013. Dipeptidyl peptidase 4 is a functional receptor for the emerging human coronavirus-EMC. *Nature* 495:251–254. <http://dx.doi.org/10.1038/nature12005>.
- Matsuno O, Miyazaki E, Nureki S, Ueno T, Ando M, Kumamoto T. 2007. Soluble CD26 is inversely associated with disease severity in patients with chronic eosinophilic pneumonia. *Biomark. Insights* 1:201–204.
- Ikushima H, Munakata Y, Iwata S, Ohnuma K, Kobayashi S, Dang NH, Morimoto C. 2002. Soluble CD26/dipeptidyl peptidase IV enhances transendothelial migration via its interaction with mannose 6-phosphate/insulin-like growth factor II receptor. *Cell. Immunol.* 215:106–110. [http://dx.doi.org/10.1016/S0008-8749\(02\)00010-2](http://dx.doi.org/10.1016/S0008-8749(02)00010-2).
- Corman VM, Eckerle I, Bleicker T, Zaki A, Landt O, Eschbach-Bludau M, van Boheemen S, Gopal R, Ballhause M, Bestebroer TM, Muth D, Müller MA, Drexler JF, Zambon M, Osterhaus AD, Fouchier RM, Drosten C. 2012. Detection of a novel human coronavirus by real-time reverse-transcription polymerase chain reaction. *Euro Surveill.* 17(39): pii=20285. <http://www.eurosurveillance.org/ViewArticle.aspx?ArticleId=20285>.
- Abbas-Terki T, Blanco-Bose W, Déglon N, Pralong W, Aebischer P. 2002. Lentiviral-mediated RNA interference. *Hum. Gene Ther.* 13:2197–2201.
- Yokoyama U, Minamisawa S, Quan H, Akaike T, Jin M, Otsu K, Ulucan C, Wang X, Baljinnayam E, Takaoka M, Sata M, Ishikawa Y. 2008. Epac1 is upregulated during neointima formation and promotes vascular smooth muscle cell migration. *Am. J. Physiol. Heart Circ. Physiol.* 295: H1547–H1555. <http://dx.doi.org/10.1152/ajpheart.01317.2007>.
- Ulucan C, Wang X, Baljinnayam E, Bai Y, Okumura S, Sato M, Minamisawa S, Hirotani S, Ishikawa Y. 2007. Developmental changes in gene expression of Epac and its upregulation in myocardial hypertrophy. *Am. J. Physiol. Heart Circ. Physiol.* 293:H1662–H1672. <http://dx.doi.org/10.1152/ajpheart.00159.2007>.
- Scobey T, Yount BL, Sims AC, Donaldson EF, Agnihotram SS, Menachery VD, Graham RL, Swanstrom J, Bove PF, Kim JD, Grego S, Randell SH, Baric RS. 2013. Reverse genetics with a full-length infectious cDNA of the Middle East respiratory syndrome coronavirus. *Proc. Natl. Acad. Sci. U. S. A.* 110:16157–16162. <http://dx.doi.org/10.1073/pnas.1311542110>.
- Yin Z, Chen YL, Schul W, Wang QY, Gu F, Duraiswamy J, Kondreddi RR, Niyomrattanakit P, Lakshminarayana SB, Goh A, Xu HY, Liu W, Liu B, Lim JY, Ng CY, Qing M, Lim CC, Yip A, Wang G, Chan WL, Tan HP, Lin K, Zhang B, Zou G, Bernard KA, Garrett C, Beltz K, Dong M, Weaver M, He H, Pichota A, Dartois V, Keller TH, Shi PY. 2009. An adenosine nucleoside inhibitor of dengue virus. *Proc. Natl. Acad. Sci. U. S. A.* 106:20435–20439. <http://dx.doi.org/10.1073/pnas.0907010106>.
- Manvar D, Singh K, Pandey VN. 2013. Affinity labeling of hepatitis C virus replicase with a nucleotide analogue: identification of binding site. *Biochemistry* 52:432–444. <http://dx.doi.org/10.1021/bi301098g>.
- Wu R, Smidansky ED, Oh HS, Takhampunya R, Padmanabhan R, Cameron CE, Peterson BR. 2010. Synthesis of a 6-methyl-7-deaza analogue of adenosine that potently inhibits replication of polio and dengue viruses. *J. Med. Chem.* 53:7958–7966. <http://dx.doi.org/10.1021/jm100593s>.
- Oh CH, Liu LJ, Hong JH. 2010. Design and synthesis of dually branched 5'-norcarboxylic adenosine phosphonodiester analogue as a new anti-HIV prodrug. *Nucleosides Nucleotides Nucleic Acids* 29:721–733. <http://dx.doi.org/10.1080/15257770.2010.509645>.
- Kameoka J, Tanaka T, Nojima Y, Schlossman SF, Morimoto C. 1993. Direct association of adenosine deaminase with a T cell activation antigen, CD26. *Science* 261:466–469. <http://dx.doi.org/10.1126/science.8101391>.
- Gracia E, Farré D, Cortés A, Ferrer-Costa C, Orozco M, Mallol J, Lluís C, Canela EI, McCormick PJ, Franco R, Fanelli F, Casadó V. 2013. The catalytic site structural gate of adenosine deaminase allosterically modu-

- lates ligand binding to adenosine receptors. *FASEB J.* 27:1048–1061. <http://dx.doi.org/10.1096/fj.12-212621>.
35. Dong RP, Tachibana K, Hegen M, Munakata Y, Cho D, Schlossman SF, Morimoto C. 1997. Determination of adenosine deaminase binding domain on CD26 and its immunoregulatory effect on T cell activation. *J. Immunol.* 159:6070–6076.
36. Raj VS, Smits SL, Provacia LB, van den Brand JM, Wiersma L, Ouwendijk WJ, Bestebroer TM, Spronken MI, van Amerongen G, Rottier PJ, Fouchier RA, Bosch BJ, Osterhaus AD, Haagmans BL. 2013. Adenosine deaminase acts as a natural antagonist for dipeptidyl peptidase 4 mediated entry of the Middle East respiratory syndrome coronavirus. *J. Virol.* <http://dx.doi.org/10.1128/JVI.02935-13>.
37. Tseng CTK, Tseng J, Perrone L, Worthy M, Popov V, Peters CJ. 2005. Apical entry and release of severe acute respiratory syndrome-associated coronavirus in polarized Calu-3 lung epithelial cells. *J. Virol.* 79:9470–9479. <http://dx.doi.org/10.1128/JVI.79.15.9470-9479.2005>.